www.amlett.org, www.amlett.com, DOI: 10.5185/amlett.2012.icnano.102
"ICNANO 2011" Special Issue Published online by the VBRI press in 2012

Calculation of lattice thermal conductivity of suspended GaAs nanobeams: Effect of size dependent parameters

S. M. Mamand[1,*], M. S. Omar[2] and A. J. Muhammed[3]

[1]*Department of physics, College of Science, University of Sulaimani, Sulaimanyah, Iraqi Kurdistan, Iraq*

[2]*Department of physics, College of Science, University of Salahaddin, Arbil, Iraqi Kurdistan, Iraq*

[3]*Department of physics, College of Science, University of Kirkuk, Kirkuk, Iraq*

[*]Corresponding author. E-mail: soran.mamand@univsul.net

ABSTRACT

Theoretical calculations of the magnitude and temperature variation of the measured thermal conductivity of undoped and doped GaAs nanobeams will present. The calculations have been performed by employing modified Callaway's theoretical model. In the model, both longitudinal and transverse modes are explicitly taken into account. Scattering of phonons is assumed to be by nanobeam boundaries, imperfections, dislocations, electrons, and other phonons via both normal and Umklapp processes. A method is used to calculate the Debye temperature and phonon group velocities for undoped and doped nanobeams from their related melting points. Phonon confinement and size effects as well as the role of dislocation in limiting thermal conductivity are investigated. The drop in thermal conductivity of doped nanobeams compared to that of the undoped beams arises from electron-phonon scattering and additional phonon scattering from a large number of point impurities due to the presence of dopant atoms. Effect of Gruneisen parameter, surface roughness, and dislocations are successfully used to correlate the calculated values of lattice thermal conductivity to that of the experimentally measured curves. Copyright © 2012 VBRI press.

Keywords: Nanostructures; lattice thermal conductivity; GaAs; phonon scatterings; lattice defects; surface roughness.

Soran M. Mamand has a Ph.D in theoretical semiconductor physics, in the University of Sulaimani in Iraq. Since 2002, he is a lecturer in physics Department, faculty of Science, university of Sulaimani. He was one of the first founders of the college of Basic Education, university of Sulaimani and he worked as an assistant of the Dean at this College, since 2003, till 2008 as well as he had worked as a head of the Mathematic and Computer Dept. from 2003 till 2006. His interest is on structure and thermal properties of nanostructure crystals.

M. S. Omar is a professor in solid state physics in the University of Salahaddin-Erbil in Iraq. His PhD is from University of Bath, England, 1985 with a thesis title "*Crystal Growth and Characterization of I-IV_2-V_3 Semiconductor Compounds and alloys based thereon*". Since then, He is leading a group working on structure and physical properties of semiconductors. In the last ten years, He is involved in working on structure and thermal properties of nanoscaled crystals, particularly Si, GaAs and GaN nanowires. His present work is on structure parameters and melting temperature of low scaled nanocrystals of solids. He and with his group, published more than 46 scientific articles in national and international journals.

Abdulkader Jaleel Muhammad was born in Kirkuk, Iraq, in 1950. He received the B.S. and M.S. degrees in physics from University of Baghdad, Iraq, in 1971, and 1978, respectively. He obtained the Ph.D. degree in Electronic Materials and Devices, from Department of Electrical & Electronic Engineering, University of Leeds, UK, in 1984. He is married and father of four boys and one girl. He worked as a staff member in Universities in Iraq. From 1985-1990 he worked as a senior scientist in a Scientific Research Center in Baghdad, Iraq. From 1995-2005 he was an Assistant professor in department of electrical and electronic engineering, University of Garyounis, Benghazi, Libya. He hold the post of the Head of the department of physics, college of science, University of Kirkuk, Kirkuk, Iraq from 2007-2011. His current interest includes electronic device physics especially MOSFETs, electrical, optical, and thermal properties of electronic materials including nanoscale materials and devices, high temperature superconductivity, solar cells and applications of photovoltaics, and power electronics.

Introduction

In nanostructure systems, thermal transport had become a subject of consideration and much interest in the area of research in the last decade [**1**]. The interest is drawn to a new thermal transport phenomenon. That is operative at these small length scales and where quantum mechanical phenomena [**2**] become significant and applied different than the bulk counterpart.

Thermal transport in the low-dimensional nano-structures (such as III-V group materials) is important for next-generation microelectronic cooling techniques, novel solid-state energy conversion devices, and micro-nanoscale sensors.

Determining the thermal conductivity of nanostructures also plays a crucial role in the development of new thermoelectric cools, which can potentially impact the thermal management of microelectronic devices. The efficiency of thermoelectric cools is determined by the figure of merit [**3**], $ZT = S^2\sigma T/(\kappa_l + \kappa_e)$, with S, σ, T, κ_l, and κ_e are the Seebeck coefficient, electrical conductivity, absolute temperature, lattice thermal conductivity, and electronic thermal conductivity, respectively. Therefore, low thermal conductivity is advantageous to the large *ZT* value. The improvements in the *ZT* value suggest the possibility of using thermoelectric coolers for thermal management of optoelectronic devices. So, the search for materials with high electrical and low thermal conductivity has increased the interest in nanoscale systems for thermoelectric application.

Fon *et al.* [**4**] achieved a direct measurement of thermal conductivity in suspended GaAs nanobeams of cross sections 100 nm × 250 nm and 150 nm × 250 nm, between 4 and 40K. They calculated the lattice thermal conductivity (LTC) on the basis of Callaway's theory [**5**]. In theoretical procedure of Fon *et al.*, they didn't consider the contribution of normal three phonon-phonon scattering processes, and neglected also contribution of polarization branches of frequency modes. However, Callaway's model considers both the normal and Umklapp forms of three-phonon interaction processes.

Barman and Srivastava [**6**], presented a theoretical investigation of the magnitude and temperature variation of the measured thermal conductivity of undoped and doped GaAs nanobeams of the measured data of Fon *et al.*. Their calculations had been performed by employing Callaway's theoretical model and Srivastava's rigorous treatment of three-phonon interactions, based on an isotropic continuum phonon dispersion relation. Barman and Srivastava's calculation didn't draw any firm conclusions about size dependent parameters (such as Gruneisen parameter, group velocity, Debye temperatures and surface roughness) of LTC of GaAs nanobeams, and their approach for calculations of the thermal conductivity is valid for relatively thick nanowires only.

In this work, we report a theoretical calculation of LTC of temperature variation and compare the numerical calculations with experimental data of Fon *et al.* Our goals are to investigate quantitatively; the effect of size dependent parameters of LTC, and investigate that our approach (in which basis on the Asen-Palmer *et al.* [**7**] approach) is general which valid for thick and thin nanobeams(or nanowires).

The rest of this paper is organized as follows. In section two, details of the theoretical background are presented. In section three we describe the result of the calculations of LTC of GaAs doped and undoped nanobeams, and comparing them with that of the experimental data, with detailed exposition to the role of the physical parameters. Conclusions are reported in the last section.

Theory

Callaway model

Callaway's phenomenological theory [**5**] which assumes a well-defined total relaxation time for the various phonon scattering processes, developed based on the Boltzmann transport equation and under the single mode relaxation time approximation, which assumes a Debye-like phonon spectrum with no anisotropies or particular structures in the phonon density of states.

The regular bulk formula for LTC (details of derivation can be found in reference [**8**] is given by:

$$\kappa = CT^3 \int_0^{\frac{\theta_D}{T}} \tau_c G(x)dx \qquad (1)$$

where:

$$C = \left(\frac{k_B}{\hbar}\right)^3 \frac{k_B}{2\pi^2 v},$$

$$G(x) = x^4 e^x \left(e^x - 1\right)^{-2}$$

$$x = \hbar\omega / k_B T$$

k_B and $\hbar$ are the Boltzmann and Planck constants respectively, ω is the phonon angular frequency, v is the phonon group velocity, τ_c is the combined (total) phonon relaxation time. θ_D is the Debye temperature, T is the absolute temperature.

Asen-Palmer *et al.* [**7**] modified this model, by treating the contribution of longitudinal and transverse phonons explicitly, and taking into account normal three phonon processes. Their approach is adopted in the present work. The LTC involves two terms $\kappa = \kappa_1 + \kappa_2$, where κ_1 and κ_2 are given by;

$$\kappa_1 = CT^3 \int_0^{\frac{\theta_D}{T}} \tau_C(x) G(x)dx \qquad (2)$$

$$\kappa_2 = CT^3 \left[\int_0^{\frac{\theta_D}{T}} \frac{\tau_C(x)}{\tau_N(x)} G(x)dx\right]^2 \left[\int_0^{\frac{\theta_D}{T}} \frac{\tau_C(x)}{\tau_N(x)\tau_R(x)} G(x)dx\right]^{-1} \qquad (3)$$

where $(\tau_c)^{-1} = (\tau_N)^{-1} + (\tau_R)^{-1}$, which τ_R is the sum of all resistive scattering processes, and τ_N is the relaxation time of normal phonon processes (N-processes). Following Callaway in dividing κ into two parts; the longitudinal κ_L and the transverse κ_T phonon branches can be expressed as:

$$\kappa = \kappa_L + 2\kappa_T \quad (4)$$

$$\kappa_L = \kappa_{L1} + \kappa_{L2} \quad (5)$$

$$\kappa_T = \kappa_{T1} + \kappa_{T2} \quad (6)$$

The partial conductivity κ_{L1} and κ_{L2} are the usual Callaway terms given by:

$$\kappa_{L1} = \frac{1}{3} C_L T^3 \int_0^{\frac{\theta_D^L}{T}} \tau_C^L(x) G(x) dx \quad (7)$$

$$\kappa_{L2} = \frac{1}{3} C_L T^3 \left[\int_0^{\frac{\theta_D^L}{T}} \frac{\tau_C^L(x)}{\tau_N^L(x)} G(x) dx \right]^2 \left[\int_0^{\frac{\theta_D^L}{T}} \frac{\tau_C^L(x)}{\tau_N^L(x)\tau_R^L(x)} G(x) dx \right]^{-1} \quad (8)$$

and similarly, for the transverse phonons;

$$\kappa_{T1} = \frac{1}{3} C_T T^3 \int_0^{\frac{\theta_D^T}{T}} \tau_C^T(x) G(x) dx \quad (9)$$

$$\kappa_{T2} = \frac{1}{3} C_T T^3 \left[\int_0^{\frac{\theta_D^T}{T}} \frac{\tau_C^T(x)}{\tau_N^T(x)} G(x) dx \right]^2 \left[\int_0^{\frac{\theta_D^T}{T}} \frac{\tau_C^T(x)}{\tau_N^T(x)\tau_R^T(x)} G(x) dx \right]^{-1} \quad (10)$$

where the superscripts L and T denoting longitudinal and transverse phonons, respectively. θ_D^L and θ_D^T are Debye temperature appropriate for longitudinal and transverse phonon branches, respectively, and;

$$C_{L(T)} = \left(\frac{k_B}{\hbar} \right)^3 \frac{k_B}{2\pi^2 \nu_{L(T)}} \quad (11)$$

where $\nu_{L(T)}$ is the longitudinal (transverse) acoustic phonon group velocities.

Phonon-scattering rates

The LTC in semiconducting crystals is limited by various mechanisms of scattering of acoustic phonons. The following phonon scattering processes are considered:

Phonon-Point defects scattering rates

The phonon–boundary scattering rate is assumed independent of temperature and frequency, for longitudinal and transverse modes can be written as [**5**]:

$$\left(\tau_B^{L(T)}\right)^{-1} = \frac{\nu_{L(T)}}{L_{eff}} \quad (12)$$

where L_{eff} is the effective phonon mean free path(MFP), for $T << \theta_D$ it is of the order of the cross-sectional dimensions, which is called Casimir length(L_C). For a cylinder with radius R, this length is equal to 2R, while for a rectangular cross-section with sides A and B, L_C =1.12(AB)$^{0.5}$.

A precise determination of L_{eff} is crucial for correctly describing the $\kappa(T)$ curve in the low temperature range. In this work, L_{eff} is equal to 7.3 mm for the best fit to the T^3 dependence of thermal conductivity at very low temperatures of the bulk sample [**9**].

Three phonon-phonon umklapp and normal scattering processes

For phonon-phonon interactions, we will assume only three-phonon processes. This is justified, as the scattering rate for four-phonon processes is two to three orders of magnitude smaller than that of three phonon processes [**10**]. For longitudinal and transverse phonons, the relaxation time in terms of the dimensionless variable x due to the three phonon Umklapp scattering rate is given by the formula [**11**]:

$$\left[\tau_U^{L(T)}(x)\right]^{-1} = B_U^{L(T)} \left(\frac{k_B}{\hbar} \right)^2 x^2 T^3 e^{-(\theta_D^{L(T)}/bT)} \quad (13)$$

where B_u is the Umklapp parameter strength given by:

$$B_U^{L(T)} = \frac{\hbar \gamma_{L(T)}^2}{M \nu_{L(T)}^2 \theta_D^{L(T)}}$$

γ is the unharmonicity parameter called Gruneisen parameter which is the measure of the crystal unharmonicity. In this work, γ is used as an adjustable parameter, as often used in the literature [**6, 12**]. For best fit it is found that, γ_L =1.85 and γ_T =1.8 for bulk GaAs in this work. In the expression above, M is the average atomic mass, b is adjustable fitting parameter, it has been reported that the value of b is in the range of 2≤ b≤ 3 for crystalline solids [**13**]. Throughout the method trail and error, the value of b is adjusted such that the best fit for calculated LTC to the experimental data is obtained, it is found to be equal to 2.5 for GaAs in this calculation.

The phonon group velocity, ν, of zincblende GaAs structure, Along [100] direction, for the longitudinal and transverse mode, are given by [**14**]:

$$\nu_L = (C_{11}/\rho)^{0.5} \quad (14)$$

$$\nu_T = (C_{44}/\rho)^{0.5} \quad (15)$$

where C_{11} and C_{44} are bulk elastic constants at 300K, and ρ is the density. The bulk longitudinal (θ_D^L) and transverse (θ_D^T) Debye temperature values were used are 440K and 320K, respectively. The total value of Debye temperature (θ_D) found by the relation $3(\theta_D)^{-3} = (\theta_D^L)^{-3} + 2(\theta_D^T)^{-3}$, is equal to 345K [**15**].

Although normal scattering processes (N-processes) is not a resistive process, but it has an important influence by transferring energy between different modes. The relaxation rates of N-processes in the Herring treatment [**16**] is given by:

$$\left[\tau_N(\omega)\right]^{-1} = B_N \omega^e T^f \quad (16)$$

where e and f are used as adjustable parameters without regard to their dependence on the properties of a given crystal. In this work, we have considered the cases (e, f) = (2,3) and (e, f) = (1,4) for longitudinal and transverse phonons, respectively [**12**]. Thus, the relaxation rates in terms of the dimensionless variable x be come as follows [**16**];

$$\left[\tau_N^L(x)\right]^{-1} = B_N^L \left(\frac{k_B}{\hbar}\right)^2 x^2 T^5$$

$$\left[\tau_N^T(x)\right]^{-1} = B_N^T \left(\frac{k_B}{\hbar}\right) x\, T^5 \quad (17)$$

$$B_N^L = \frac{k_B^3 \gamma_L^2 V_o}{M\hbar^2 \nu_L^5}, \qquad B_N^T = \frac{k_B^4 \gamma_T^2 V_o}{M\hbar^3 \nu_T^5},$$

and V_o is the volume per atom of the crystal.

Phonon-impurity scattering rate

Two types of point defects are considered, isotope and foreign (impurity) atoms. According to Klemens [**17**] approach, the relaxation rate for point defect scattering is given by:

$$\left[\tau_p\right]^{-1} = I\omega^4 \quad (18)$$

where I is the point defect strength parameter, which at least is the sum of two terms $I = I_{iso} + I_{imp}$,where I_{iso} being due to the scattering by distribution of isotopes of the elements in the compound, and I_{imp} being due to the scattering caused by foreign atoms(impurity).

Phonon-isotope scattering rate

For longitudinal and transverse modes, the phonon-isotope scattering rate in terms of the dimensionless variable x become as [**17**]:

$$\left[\tau_{iso}^{L(T)}(x)\right]^{-1} = I_{iso}^{L(T)} \left(\frac{k_B}{\hbar}\right)^4 x^4 T^4 \quad (19)$$

$$I_{iso}^{L(T)} = \frac{V_o}{4\pi \nu_{L(T)}^3} \Gamma \quad ,$$

Γ is the measure of the strength of the mass-difference scattering defined as:

$$\Gamma = \sum_i c_i \left[\frac{m_i - \overline{m}}{\overline{m}}\right]^2 \quad (20)$$

with $\overline{m} = \sum_i c_i m_i$, where m_i is the atomic mass of the i^{th} isotope and c_i is the fraction atomic natural abundance. For a binary compound composed of two different elements, A and B, Γ is given as [**12**]:

$$\Gamma(AB) = 2\left[\left(\frac{M_A}{M_A + M_B}\right)^2 \Gamma(A) + \left(\frac{M_B}{M_B + M_A}\right)^2 \Gamma(B)\right] \quad (21)$$

where M_A is the average atomic mass of A , and M_B is that of B. The factor 2 in front of the square brackets is due to the fact that AB is a binary compound [**12**]. The value of Γ for GaAs is calculated from the isotope compositions of Ga (of 60.1% of ^{69}Ga and 39.9% of ^{71}Ga) and As (100% of most stable ^{75}As) and is equal to 0.9254×10^{-4}.

Lattice thermal conductivity of nanostructure

The longitudinal and transverse modes of the phonon-impurity scattering rate in terms of the dimensionless variable x become as [**17**]:

$$\left[\tau_{imp}^{L(T)}(x)\right]^{-1} = I_{imp}^{L(T)} \left(\frac{k_B}{\hbar}\right)^4 x^4 T^4 \quad (22)$$

$$I_{imp}^{L(T)} = \frac{3V_o^2 S^2}{\hbar \nu_{L(T)}^3} N_{imp} ,$$

S is the scattering factor which usually has a value close to unity [**17**], and N_{imp} is the impurity concentration.

Phonon- dislocation scattering rate

Phonons will scatter on dislocations by two distinctive mechanisms. The first mechanism is scattering of phonons on the core of the dislocation lines, which is a short-range interaction. The second mechanism is scattering of phonons by the elastic strain field of dislocation lines, which is a long-range interaction.

The phonon scattering rate at the core of the dislocation is given by [**18**]:

$$\left[\tau_{DC}(\omega)\right]^{-1} = \eta N_D \frac{V_o^{4/3}}{v^2}\omega^3 \qquad (23)$$

where N_D is the density of the dislocation lines of all types, and η is the weight factor to account for the mutual orientation of the direction of the temperature gradient and the dislocation line, the average value found by integration is η =0.55 [**17**]. For longitudinal and transverse mode in terms of the dimensionless variable x, Eq. (23) becomes:

$$\left[\tau_{DC}^{L(T)}(x)\right]^{-1} = \eta N_D \frac{V_o^{4/3}}{v_{L(T)}^2}\left(\frac{k_B T}{\hbar}\right)^3 x^3 \qquad (24)$$

The phonon scattering rate by the elastic field of screw $(1/\tau_{DS})$, edge $(1/\tau_{DE})$ and mixed dislocation $(1/\tau_{DM})$ are given by [**17, 18**]:

$$\left[\tau_{DS}\right]^{-1} = \frac{2^{3/2}}{3^{7/2}}\eta N_D^S b_S^2 \gamma^2 \omega \qquad (25)$$

$$\left[\tau_{DE}\right]^{-1} = \frac{2^{3/2}}{3^{7/2}}\eta N_D^E b_E^2 \gamma^2 \omega \left\{\frac{1}{2}+\frac{1}{24}\left(\frac{1-2\upsilon}{1-\upsilon}\right)^2\left[1+\sqrt{2}\left(\frac{v_L}{v_T}\right)^2\right]^2\right\} \qquad (26)$$

$$\left[\tau_{DM}\right]^{-1} = \frac{2^{3/2}}{3^{7/2}}\eta N_D^M \gamma^2 \omega \left(b_S^2 + b_E^2\left\{\frac{1}{2}+\frac{1}{24}\left(\frac{1-2\upsilon}{1-\upsilon}\right)^2\left[1+\sqrt{2}\left(\frac{v_L}{v_T}\right)^2\right]^2\right\}\right) \qquad (27)$$

where, $\upsilon = C_{12}/(C_{11}+C_{12})$ is Poisson's ratio(C_{11} and C_{12} are elastic constants). b_S , b_E and b_M are magnitudes of Burger vectors for the screw, edge, and mixed dislocations, respectively, which $b_M = b_s + b_E$. In this work it is assumed that the values of these Burger vectors are equal; and b_S = b_E = 0.399 nm [**19, 20**]. The total density of dislocation is $N_D = N_D^S + N_D^E + N_D^M$, where N_D^S, N_D^E and N_D^M are the densities for the screw, edge and mixed dislocations, respectively. The assumption of equally distributed dislocations among the possible types is a feasible one [**21**], so in the present work, $N_D^S = N_D^E = N_D^M$ would be assumed.

Assuming that phonon relaxation on dislocations is an independent process, the combined phonon relaxation can be written as $1/\tau_D = \sum_j 1/\tau_j$, where τ_j represents scattering times on the dislocation core, on the elastic strain field of screw, edge and mixed dislocations.

By substitution of the parameters for the scattering rates of screw, edge and mixed dislocations, longitudinal and transverse mode of the combined relaxation rate in terms of the dimensionless variable x become:

$$\left[\tau_{DSEM}^{L(T)}(x)\right]^{-1} = 0.6*10^{-20} N_D \gamma_{L(T)}^2 \frac{k_B T}{\hbar} x \qquad (28)$$

Phonon-electron scattering rate

Acoustic phonon scattering rates on electrons of longitudinal and transverse mode in terms of the dimensionless variable X, are given by [**8**]:

$$\left[\tau_{ph-e}^{L(T)}(x)\right]^{-1} = \frac{n_e E^2 x}{\rho v_{L(T)}^2 \hbar}\sqrt{\frac{\pi m^* v_{L(T)}^2}{2k_B T}} \times \exp\left(-\frac{m^* v_{L(T)}^2}{2k_B T}\right) \qquad (29)$$

where, n_e is the concentration of conduction electrons, E is the deformation potential, ρ is the mass density, m^* is the effective mass of the electron. E =8.6 eV and m^* =0.067 m_e, where m_e is the electron rest mass [**6**]. Assuming that, the phonon confinement does not strongly affect phonon-electron scattering rates [**8**]. Finally the total combined relaxation rate is:

$$\left[\tau_C^{L(T)}\right]^{-1} = \sum_s \left[\tau_s^{L(T)}\right]^{-1} \qquad (30)$$

where, $\tau_s^{L(T)}$ represent the scattering times on the Umklapp and normal processes, impurity, boundary, core dislocation, elastic field (screw, edge, and mixed), and phonon-electron.

Lattice thermal conductivity of nanostructure

Theoretical and experimental investigation demonstrates a size-dependent behavior of lattice vibration of nanostructures [**22**]. The high surface-to-volume ratio of semiconductor nanostructures can dramatically alter the fundamental properties with respect to the corresponding bulk samples. Size can be therefore considered a key parameter, controlling the material properties as well as subsequent performance of the device.

Balandin and Wang [**2**] have demonstrated that acoustic phonon dispersion relations in nanostructures can be modified from the bulk due to the phonon confinement effect. The phonon confinement (which causes to reduce phonon group velocity), however, can lead to considerable reduction of LTC in nanostructures [**1, 2**].

The size dependent parameters should be carefully accounted for. These parameters are; v , θ_D , ε (surface

roughness), γ and lattice dislocations density(N_D). Following references [**23, 24**], assuming the system to be isotropic, the relation between group velocity (ν) and Debye temperature (θ_D) for nanostructure with that of bulk is given as:

$$\frac{\nu^n}{\nu^B} = \frac{\theta_D^n}{\theta_D^B} \qquad (31)$$

where the superscript n and B are refer to nanostructure and bulk ,respectively.

The Debye temperature can be obtained from Lindemann's relation of melting criterion [**25**], and the modern form of this relation for θ_D is given by [**26, 27**]:

$$\theta_D = const.\left(\frac{T_m}{MV_o^{2/3}}\right)^{1/2} \qquad (32)$$

where M is the molar mass. Adopting the same relation for nanostructures, the following relation can be introduced:

$$\left(\frac{\theta_D^n}{\theta_D^B}\right)^2 = \frac{T_m^n}{T_m^B} \qquad (33)$$

where T_m^n is the melting point of the nanostructure. The melting point of the nanostructure is depends on the dimensions (size dependent) and can be calculated from the relation [**26, 28**]:

$$\frac{T_m^n}{T_m^B} = \exp\left(-\frac{2(S_m - R)}{3R[(r_n / r_o) - 1]}\right) \qquad (34)$$

where r_o is a critical radius at which almost all atoms of a crystal are located on its surface of bulk , r_n is a radius of nanobeams. The parameter r_o depends on the structure dimension d , the relation between r_o and d is [**28**]:

$$r_o = (3 - c)d \qquad (35)$$

where c = 0 ,1 ,and 2 for a nanoparticles, nanowire(nanobeams), and thin films, respectively [**28,29**]. d is atomic/molecular diameter and its value is equal to 0.245 nanometer for GaAs [**30**]. S_m and R are the bulk overall melting entropy and ideal gas constant, respectively. $S_m = H_m / T_m$, where H_m is enthalpy of formation. Employing the data given in **Table 1**, values for T_m^n , θ_D^n, and ν^n are calculated through the use of equations (31) to (35), and the results are summarized in table 2, in which their values decreases as the diameter of nanostructure decrease [**1,2**]. These values will be used in the rest of the present calculations.

The boundary scattering for nanostructures is modified as follow; LTC at very low temperatures, depends linearly on the sample dimension when the scattering is strictly diffuse [**31**]. The effective phonon MFP would be modified as [**32**]:

$$\frac{1}{L_{eff}} = \frac{1}{L_C} + \frac{1}{l} \qquad (36)$$

Table 1. Material parameters of GaAs.

Lattice constant (nm)	a	0.56533	[**33**]
Volume per atom (m^3)	V_o	$22.6*10^{-30}$	[**34**]
Average atomic mass (kg)	M	$120*10^{-27}$	[**33**]
Density (kg/m^3)	ρ	5317	[**35**]
Elastic constants (GPa)	C_{11}	118.8	[**36**]
	C_{12}	53.8	[**36**]
	C_{44}	59.4	[**36**]
Melting point (K)	T_m	1511	[**37**]
Enthalpy (KJ/mol)	H_m	120	[**38**]

Assuming partial specular reflection of phonons, the relaxation rates of boundary scattering (Eq. 12) for longitudinal and transverse modes can be rewritten as [**32**]:

$$\left[\tau_B^{L(T)}\right]^{-1} = \nu_{L(T)}\left(\frac{1}{L_C}\frac{(1-\varepsilon)}{(1+\varepsilon)} + \frac{1}{l}\right) \qquad (37)$$

$$\frac{1}{L_{eff}} = \left(\frac{1}{L_C}\frac{(1-\varepsilon)}{(1+\varepsilon)} + \frac{1}{l}\right)$$

ε is specularity parameter, which represents the probability that the phonon is undergoing a specular scattering event at the interface [**8**]. The value of 1- ε represents the probability that the phonon is undergoing a diffuse scattering event. ε is between 0 and 1 , with ε =0 representing a purely rough surface and ε =1 representing a purely smooth surface, and l is the length of the samples. For the present GaAs nanobeam samples, l is equal to 6 micrometers [**4**]. In this work, to achieve the best fit of calculated LTC to that of the experimental data just below maximum value of the conductivity, ε will be treated as an adjustable parameter.

Results and discussion

For purposes of comparison, and to point out the importance of N-processes, the response of bulk phonons will be presented first. The result of calculations for temperature dependence of LTC in the temperature range 2 ≤ *T*≤ 300 K, for bulk Zincblend GaAs samples are presented in **Fig. 1**, using equations (3-30). The material parameters of bulk Zincblend GaAs used in the calculations are summarized in **Table 1**. The symbols (circles) are experimental data taken from reference [**9**].

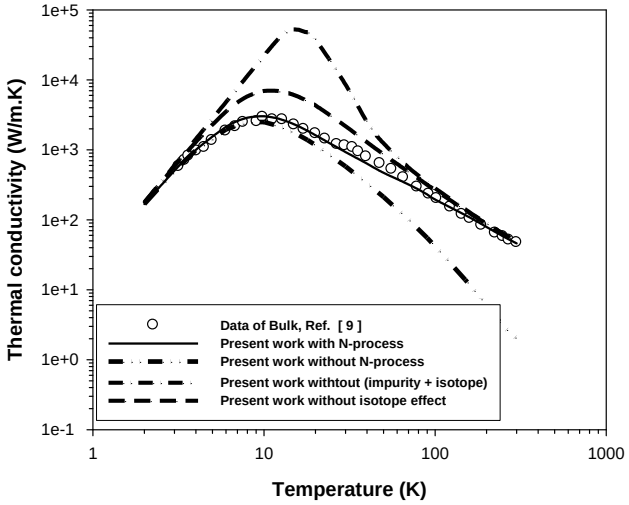

Fig. 1. Temperature variation of LTC of bulk GaAs. Open circlesare data from Ref. [9].

Table 2. Calculated melting point, Debye temperature, and group velocity for undoped and doped nanobeams. Melting point calculated from Eq. (34). Debye temperature calculated from Eq. (33), and group velocity calculated from Eq. (31) for nanobeams. Bulk group velocity from Eqs. (14) and (15).

Crystal	Melting point (K)	θ_D^L (K)	θ_D^T (K)	v_L (m/sec)	v_T (m/sec)
Bulk	1511	440	320	4730	3340
Doped nanobeam	1477	434.34	315.9	4669.1	3297.2
Undoped nanobeam	1467	433.1	314.9	4655.8	3287.4

The solid line is the present theoretical work with the effect of N-processes included; the dash-dot-dot line is the present theoretical work without N-processes. A comparison of these two lines with the experimental data indicates the importance of the N- processes. The present result suggests that the K_2 term (N-processes) is important and cannot be neglected in spite of its small value compared to defect and Umklapp scattering.

In the same figure the effect of isotope and impurity scattering are disclosed; the dash-dotted line is the present theoretical work without both isotope and impurity contribution, while the dashed line is the present theoretical work without isotope contribution only. Comparing these curves with the experimental data indicates the importance of these mechanisms especially in the mid-temperature range around the peak in the conductivity curve [**17, 39**]. **Fig. 2** displays a comparison of the experimental data taken from references [**4,9**] with the present theoretical calculation (solid lines) in the temperature range 2–300 K, for the temperature variation of the thermal conductivity of doped and undoped nanobeams as well as for bulk samples. The experimental data for nanobeams are from reference [**4**], and that for the bulk is from reference [**9**].

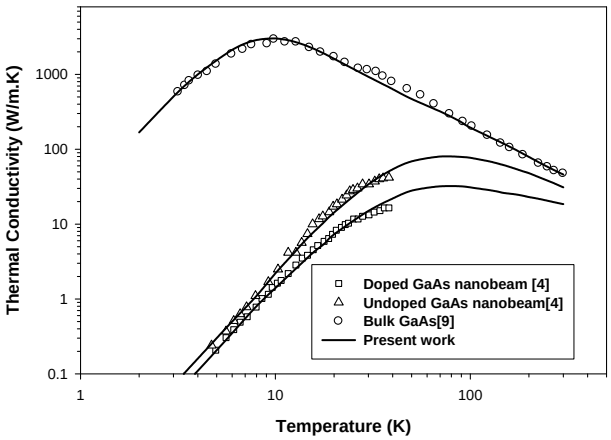

Fig. 2. Temperature variation of the thermal conductivity of bulk GaAs, and undoped and doped GaAs nanobeams. Lines are the present theoretical results and symbols are the experi- mental results from reference[9] for bulk and the nanobeams from reference [4].

The fitting for all the cases considered is good. This had been performed by using the values of θ_D and v for bulk and nanobeams (from **Table 2**), and the values of adjustable parameters, γ, ε, N_D, and L_{eff} (which presented in **Table 3**) were adjusted such that to obtain the best fit. The temperature dependence of the thermal conductivity of the nanobeams can be described as follows: Boundary effect would control the phonon scattering at very low temperatures, in which depend on the size and surface quality [**8, 40**]. In our calculations, by using the Casimir limit (L_C) [**31**] equal to the size of the nanobeams (see **Table 3**), and specularity parameter (ε) was used to model the surface roughness, they are combined through the use of Eq. (37). Good fit to the experimental data of reference [**4**] was achieved. Values of ε given in **Table 3**, indicate that each phonon is specularly reflected on an average of (1/1-ε) ≈ 3 and 2 times for undoped and doped beams respectively, before being diffusely scattered. Thus, the increased rate of diffuse boundary scattering, i.e. the size effect, is actually responsible for the shift in the conductivity peak towards a higher temperature and in the reduction of the magnitude of thermal conductivity of the nanobeam compared to that of the bulk GaAs crystal [**6**].

Table 3. The fitting parameters of GaAs bulk and nanobeams used in calculating LTC, and calculated LTC at 300K.

Crystal	ε	L_c (m)	$L_{effc.}$ (μm)	γ_L	γ_T	$N_{imp.}$ *1024 (m-3)	N_D *1015 (m-2)	n_e *1021 (m-3)	κ (W/m.K) At 300K
Bulk	0	0.0073	7300	1.85	1.8	0.05	0	0	46
Undoped Beam	0.7	177*10-9	0.85	1.98	1.94	0	2.0	0	31
Doped Beam	0.47	216*10-9	0.55	1.91	1.86	5	5.9	1.5	18.5

The increased level of impurity centers in the doped nanobeam, apparently leads to a value of ε smaller than that of the undoped nanobeam (see **Table 3**), this effect can be explain as follows: According to Ziman [**40**], ε is related to phonon wave vector $\vec{k}$, and asperity parameter, P, by $\varepsilon(\vec{k}) = \exp[(-2\vec{k}P\cos\Phi)^2]$. Where P is the root mean square height deviation in the surface and Φ is the angle of phonon incident. The larger value of ε corresponds to the smaller roughness(smaller P), i.e. the smoother surface, thus the more probability of specular scattering, vice versa, the smaller ε corresponds to the more probability of diffusive scattering. Thus, the smaller value of ε for the doped beam corresponds to a higher value of P, which can arise from the presence of different atoms on the surface of the doped beam. These results are related to the phonon mean free path in various conditions, which suggests that dense surface features may enhance surface scattering thereby hindering phonon transport and decreasing LTC [**41**].

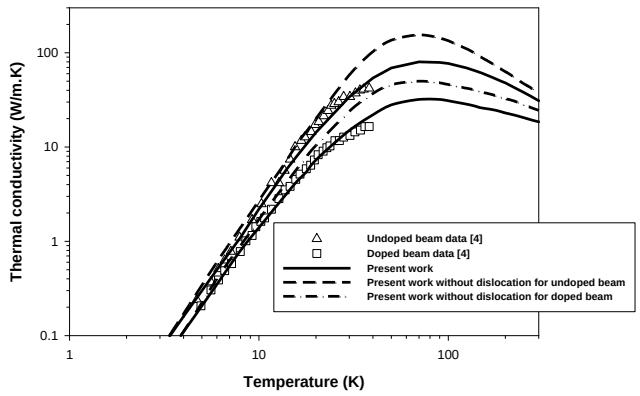

Fig. 3. Calculated LTC of undoped and doped beams. Dashed and dash-dotted lines are without dislocations for undoped and doped beams, respectively.

Presence of impurity in addition to electron-phonon scattering will be responsible for decreasing lattice thermal conductivity of doped nanobeam compare to that of undoped [**4**]. The point defect scattering rate increases approximately 10 times compared to that for the undoped beam, due to the presence of dopant atoms in the doped beams [**6**]. The concentration of electron is found to be equal to 1.5×10^{21} m^{-3}, because the doped beams are not uniformly doped, as only the topmost 50 nm layer is doped, the scattering of electrons with phonons would be effective only at very low temperatures.

The role of isotope scattering was tested in undoped beam. It can be shown that there is only 8% contribution to the lattice thermal conductivity from 10K and above, unlike the bulk in which there is a contribution of about 57% around maximum conductivity, because the boundary scattering in nanobeams has a very strong influence on thermal conductivity up to about a temperature of 100 K [**6**]. This means that, lattice thermal conductivity of nanobeams is limited by imperfections (dislocation and impurity) as well as phonon-phonon processes at intermediate and high temperature.

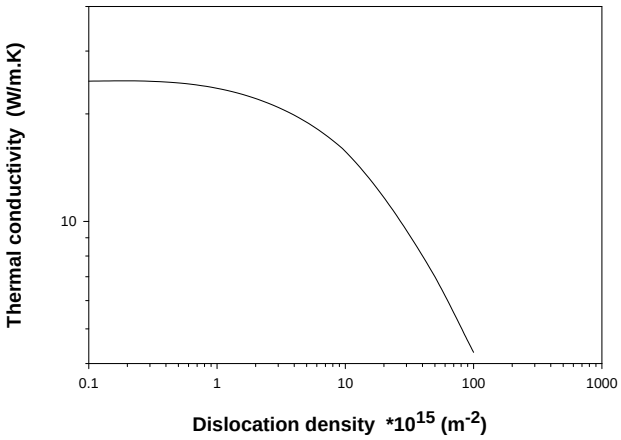

Fig. 4. Theoretical calculation of LTC as a function of dislocation line density for doped GaAs nanobeam at 300K.

The density of dislocation lines (N_D), have significant role in limiting LTC of nanostructures [**42**]. This is evident from **Fig. 3** in which recalculations of LTC are performed without the effect of dislocation line density for both doped and undoped nanobeams. In both cases, inclusion of dislocations in the calculations (the solid lines), results in a better fit to the experimental data. Dislocations will increase with increasing of impurity [**35**]. The doped beam

has higher dislocations due to impurities (see **Table 3**).There is interaction between the localized impurity atoms and the strain field in the vicinity of the dislocations.

Fig. 4 shows calculated LTC as a function of N_D for the doped nanobeam GaAs at room temperature. It is obvious from **Fig. 4,** that LTC is almost independent of N_D for low densities (below 10^{14} m^{-2}), but it becomes strongly dependent on N_D for higher densities. For N_D < 10^{14} m^{-2} LTC does not depend on N_D which means that it is determined by intrinsic properties, e.g., phonon-phonon, and point defect scattering [**21**]. This result is in a good agreement with those reported previously for GaN films [**21, 43**].

At room temperature, which the phonon-phonon scattering has significant role in limiting thermal conductivity [**11**], the Gruneisen parameter (γ) which is a measure of the crystal unharmonicity, seems to be increase as the cross section of the beams decrease (see **Table 3**). Due to the lack of the data of smaller diameter, this change may be in doubt. Nevertheless, the increase of Gruneisen parameter as the diameter decrease in terms of change of Young's modulus can be explain as follows: when a crystal size reduces to a nanoscale range, the surface to bulk ratio will begin to dominate the mechanical properties of the material. The Young's modulus of single crystal material reflects physics of interatomic bond energy and lattice structure. Gruneisen parameter has a positive correlation with the bulk and Young's modulus [**44**], so an increase in bulk and Young's modulus (as the cross section of nanostructures decrease) is expected to reflect itself an increase in Gruneisen parameter. Recently, Wang *et al.* [**45**] were used *in situ* transmission electron microscopy nanocompression technique and finite element analysis to investigate the mechanical behavior of GaAs nanowires. They inferred that, the Young's modulus of GaAs nanowires will increase as the diameter decrease. This result is agree with that observed in [111] Silicon nanowires [**42**] and ZnO nanowires [**46**].

Barman and Srivastava [**6**] was used the same value of γ (=1.8), for bulk and nanobeams, this will be in contrast to the results of the present work and that of Wang *et al.* [**45**]. Mechanical properties of nanostructures are different from that of the bulk counterparts [**45-48**]. So, variation of the parameters of the nanostructure materials should be carefully taking into account.

Conclusion

Theoretical calculations of LTC for suspended GaAs nanobeams of cross sections 100 × 250 and 150 × 250 nm are reported. Reduction of the LTC of the beams is due to large boundary scattering effect and phonon confinement, in which the former causes to increase thermal resistance, and the latter causes to reduce phonon group velocities. The phonon scattering on electrons and impurity in doped beam has significant effect in decreasing LTC comparing to that of the undoped beam. Results shows that the dislocation density have significant role, which is in a good agreement qualitatively with the other work in the literature. The lattice thermal conductivity would be limited by intrinsic properties and dislocation density at high temperatures, and does not depend on dislocation at density less than 10^{14} m^{-2}. Result of the values of adjustable parameters N_D , ε , L_{eff} , and γ in the correlation between theoretical and experimental curves of LTC of nanobeams indicate the significance of size dependent parameters.

Acknowledgement
Authors would like to acknowledge college of science, university of Sulaimani in Sulaimanyah, Iraq for their financial support.

Reference

1. Balandin, A, *phys. Low-Dim. Structure* **2000**, *1/2*, 1.
2. Balandin, A; and Wang, K. *Phys. Rev. B* **1998**, *58*, 1544.
3. Nolas, G.; Sharp, J.; and Goldsmid, H. *In Thermoelectrics*; Springer, New York, **2001**.
4. Fon, W.; Schwab, K.; Worlock, J; Roukes, M. *Phys. Rev. B* **2002**, *66*, 045302. **DOI:** 10.1103/PhysRevB.66.045302.
5. Callaway, J. *Phys. Rev.* **1959**, *113*, 1046. **DOI:** 10.1103/PhysRev.113.1046.
6. Barman, S.; Srivastava, G.P. *Phys. Rev. B* **2006**, *73*, 205308. **DOI:** 10.1103/PhysRevB.73.205308.
7. Asen-Palmer, M.; Bartkowski, K.; Gmelin, E.; Cardona, M.; Zhernov, A.; Inyushkin, A.; Taldenkov, A.; Ozhogin, V.; Itoh, K.; Haller, E. *Phys. Rev. B* **1997**, *56*, 9431. **DOI:** 10.1103/PhysRevB.56.9431
8. Zou, J.; and Balandin, A. *J. Appl. Phys*. **2001**, *89*, 2932. **DOI:** 10.1063/1.1345515.
9. Holland, M. G. *Phys. Rev.* **1964**, *134*, A471.
10. Ecsedy, D. J.; Klemens, P. G. *Phys. Rev. B* **1977**, *15*, 5957. **DOI:** 10.1103/PhysRevB.15.5957
11. Slack, G. A.; Galginaitis, S. *Phys. Rev.* **1964**, *133*(1A), 253.
12. Morelli, D. T.; Heremans, J. P.; and Slack, G. A.*Phys. Rev. B* **2002**. *66*,195304. **DOI:** 10.1103/PhysRevB.66.195304
13. Berman, R.; *In Thermal Conductivity in Solid*, Oxford University Press,Oxford, **1976**.
14. McSkimin, H.; Jayaraman, A.; Andreatch, P. *J. App. Phys.* **1967**, *38*, 2362.
15. Steigmeier, E. *J. Appl. Phys. Lett.* **1963**, *3(1)*, 6.
16. Herring, C. *Phys. Rev.* **1954**, *95*, 954. **DOI:** 10.1103/PhysRev.95.954.
17. Klemens, P. G. *Proc. R. Soc. London, Ser A* **1955**, *68*, 1113.
18. Klemens, P. G. *In Solid State Physics*, edited by F.Seitz and D.Turnbull; Academic, New York, **1958**, vol.7.
19. Vechten, J. V. *Phys. Rev. B* **1978**, *17*, 3197. **DOI:** 10.1103/PhysRevB.17.3197.
20. Goryunova, N. A.; *In the Chemistry of Diamond-like Semiconductors*, MIT, Cambridge, **1965**, p. 99.
21. Zou, J.; Kotchetkov, D.; Balandin, A.;Florescu, D. I.; Pollak, F. H. *J.Appl.Phys.* **2002**, *92*, 2534. **DOI:** 10.1063/1.1497704.
22. Sun, C.; Pan, L.; Li, C.; Li, S. *Phys. Rev. B* **2005**, *72*, 134301. **DOI:** 10.1103/PhysRevB.72.134301
23. Post, E. J. *Can. J. Chem.* **1953**, *31*,112.
24. Regel, A.; and Glazov, V. *Semiconductors*, **1995**, *29*, 405.
25. Lindemann, F. *Z. Phys.* **1910**, *11*, 609.
26. Liang, L.; and Li, B. *Phys. Rev. B* **2006**, *73*, 153303. **DOI:** 10.1103/PhysRevB.73.153303.
27. Dash, J.; *Rev. Mod. Phys.* **1999**, *71*, 1737. **DOI:** 10.1103/RevModPhys.71.1737.
28. Liang, L.; Shen, C.; Du, S.; Liu, W.; Xie, X.; and Gao, H. *Phys.Rev. B* **2004**, *70*, 205419. **DOI:** 10.1103/PhysRevB.70.205419
29. Zang, Z.; Zhao, M.; and Jiang, Q. *Semicond. Sci. Tech.* **2001**, *16*, L33.
30. Ohtake, A.; Tsukamoto, S.; Pristovsek, M.; and N. Koguchi, N. *Appl. Surf. Sci*. **2003**, *212-213*, 146
31. Casimir, H. *Physica* **1938**, *5*, 495.

32. Vandersande, J. W. *Phys. Rev. B* **1977**, *15*, 2355. **DOI:** 10.1103/PhysRevB.15.2355.
33. Driscoll, C. M.; Willoughby, A.; Mullin, J.; and Straughan, B. *In Gallium Arsenid and Related Compounds*, Inst. of phys. London, **1975**, p. 275.
34. Shinde, S. L.; Goela, J. S. *In High Thermal Conductivity Materials*, Springer, **2006**, p. 47.
35. Blackemore, J. S. *J. Appl. Phys.* **1982**, *53*, R123.
36. Bateman, T.; Mcskimin, H.; Whelan, J. *J. Appl. Phys*. **1959**, *30*, 544.
37. Panish, M. B. *J. Crystal Growth*, **1974**, *27*, 6.
38. Hillert, M.; Staffansson, L. *Acta Chem. Scand*. **1970**, *24*, 3618.
39. Pomeranchuck, I. *J. Phys. (USSR)* **1942**, *6*, 237.
40. Ziman, J. M. *In Electrons and Phonons*, Claredon, Oxford, **1960.**
41. Liu, L. and Chen, X. *J. Appl. Phys.* **2010**, *107*, 033501. **DOI:** 10.1063/1.3298457
42. Omar, M. S.; and Taha, H. T. *Sadhana* **2010**, *35*, 177.
43. Kotchetkov, D.; Zou, J.; Balandin, A.; Florescu, D.; and Pollak, F.; *J. Appl. Phys. Lett.* **2001**, *79*, 4316. **DOI:** 10.1063/1.1427153.
44. Iwanaga, H.; Kunishige, A.; Takenchi, S.; *J. Material Sci.* **2000**, *35*, 2451.
45. Wang, Y.; Wang, Li.; Joyce, H.; Gao, Q.; Liao, X.; Mai, Yi.; Tan, H.; Zou, J.; Ringer, S.; Gao, H.; Jagadish, Ch. *Adv. Materials* **2011**, *23*, 1356.
46. Chen, C.; Shi, Y.; Zhang, Y.; Zhu, J.; Yan, Y.; *Phys. Rev. Lett.* **2006**, *96*, 075505. **DOI:** 10.1103/PhysRevLett.96.075505.
47. Gulans, A.; and Tale, I.; *Phys. Stat. Sol (C)* **2007**, *4*, 1197.
48. Verma, S.; Yadav, R.; Yadav, A.; Joshi, B.; *Materials Lett.* **2010**, *64*, 1677.